Thi-Qar Medical Journal (TQMJ):Vol.( 27),No.(1),2024

Web Site: https://jmed.utq.edu Email: utjmed@utq.edu.iq

ISSN (Online): 3006-4791

# Radiological and Endoscopic Study of the Anatomical Landmark to Localise the Anterior Ethmoidal Artery in Endoscopic Sinus Surgery

**Muaid Ismail Aziz**[1]

**Mariwan Latif Fatah**[2]

**Haval Ahmed Hama**[3]

**Omer Sherko Omer**[4]

1 University of Sulaimani College of Medicine, Branch of Clinical Science

2 University of Sulaimani College of Medicine, Branch of Clinical Science and Smart Health Tower

3 University of Sulaimani College of Medicine, Branch of Clinical Science

4 Sulaimani General Directorate of Health, ENT – Head and Neck Center.

## Abstract

**Introduction:** The anterior ethmoidal artery (AEA) is an important anatomical structure during endoscopic sinus surgery (ESS) due to the risk of injury. Preoperative identification of landmarks correlating with AEA location could help reduce complications. This study aims to determine anatomical variations affecting the AEA course concerning the skull base.

**Methods:** A retrospective review was conducted of 50 patients who underwent ESS. Preoperative coronal CT scans were analysed for supraorbital ethmoid cells (SOEC), suprasellar cells (SBC), and Keros classification of olfactory fossa depth. Radiological AEA location relative to the skull base was recorded. Intraoperative videos were reviewed to correlate findings with radiology.

**Results:** SOEC were present on 24 right and 28 left sides. SBC were present in 39 right and 33 left sides. The most common Keros types were right type 1 (31) and left type 1 (27). Radiologically, AEA was within the skull base on 32 right and 27 left sides. Intraoperative correlation showed a higher incidence of AEA below the skull base with SOEC/SBC presence and

more profound Keros types. The relationship between anatomical variations and AEA location was statistically significant ($p<0.05$).

**Conclusion:** This study demonstrates that anatomical variations, including SOEC, SBC, and Keros classification, influence the course of the AEA relative to the skull base. Preoperative identification using these landmarks on CT may help surgeons localise and protect the AEA during ESS, thus reducing the risks of injury. More extensive prospective studies are needed to validate these findings.

**Keywords:** Radiological study, Endoscopic sinus surgery, Anatomical landmark, Anterior ethmoidal artery, Anterior nasal spine.

**Introduction :**The AEA is a high-risk area during ESS, as it courses along the ethmoid roof, often found in a mesentery below the skull base. Injury to the AEA can lead to severe bleeding, CSF leaks, retro-orbital hematoma, and potential complications like optic nerve compression and blindness. The embryological development of the ethmoid sinus begins around the fourth month of fetal development, with the sinus originating from multiple centres and gradually enlarging during primary pneumatisation. By the age of 12 years, the ethmoid sinus approaches adult size. The ophthalmic artery, from which the AEA originates, develops from the primitive internal carotid, stapedial, and pharyngeal artery systems, reaching its adult configuration around 40 months. The AEA is a consistent branch of the ophthalmic artery, passing through the anterior ethmoidal canal with 1 to 5 small branches. It is present in 90% of cases when the ophthalmic artery crosses over the optic nerve and 80% when it crosses under. Understanding the anatomy and variations of the AEA is crucial for safe and successful ESS (1,2).

**Anatomy of the Anterior Ethmoidal Artery :**The anterior ethmoidal artery (AEA) and posterior ethmoidal artery (PEA) are significant vessels that supply the ethmoid sinus, nasal septum, and anterior skull base. They are branches of the ophthalmic artery. The AEA typically lies between the second and third lamellae of the lateral nasal wall, posterior to the anterior face of the ethmoid bulla, and about 24 mm posterior to the anterior lacrimal crest along the frontoethmoidal suture line. It passes between the superior oblique and medial rectus muscles before exiting the orbit through the anterior ethmoid foramen and the anterior ethmoid nerve. It then crosses the cribriform plate and enters the nose through a slit adjacent to the crista galli, becoming the dorsal nasal artery. The PEA lies approximately 12 mm posterior to the AEA along the frontoethmoidal suture line, with the optic nerve about 6 mm posterior to the PEA. From anterior to posterior, the lamellae of the ethmoid sinus are the uncinate process, anterior face of the ethmoid bulla, basal lamella of the middle turbinate, superior turbinate, and anterior face of the sphenoid sinus. If the bulla lamella is absent superiorly, the anterior ethmoidal artery may be at risk during dissection of the frontal

recess, as the bulla lamella would not protect it. The artery's curved course from the orbit to the cribriform plate also increases the risk of injury (3,4).

**Supraorbital Ethmoid Cells :**Supraorbital ethmoid cells are anterior ethmoid air cells that extend superiorly and laterally over the orbital roof. These cells can cause obstruction of the frontal recess, be mistaken for the actual frontal sinus, and are associated with a low position of the anterior ethmoid artery within a mesentery. The supraorbital ethmoid cell also creates a narrow orbitofrontal aperture that can be challenging to operate within. Approximately 65% of Caucasian patients have extensively pneumatised orbital plates of the frontal bone, resulting in supraorbital ethmoid cells, with a lower incidence in East Asian populations. Coronal CT scans can reveal the 'double lamina' effect of the orbital roof due to pneumatisation, with the anterior ethmoidal artery traversing the space in a mesentery (5).

**The Keros Classification :**The Keros classification, introduced by Predrag Keros in 1962, categorises the depth of the olfactory fossa based on the height of the lateral lamella of the cribriform plate. This system divides the depth into three types: Type 1 (1-3 mm, 26.3%), Type 2 (4-7 mm, 73.3%), and Type 3 (8-16 mm, 0.5%). As seen in Type 3, a deeper olfactory fossa exposes the thin cribriform plate to risks like trauma, tumour erosion, CSF leaks, and surgical complications (6). The skull base's intricate landscape reveals a hierarchy of susceptibility to erosion and defects. Due to its delicate structure, the cribriform plate is the most vulnerable site, with 51% of cases. The sphenoid lateral pterygoid recess (31%) and ethmoid roof (8%) are also prone to issues, while the peri Sella region hints at unravelled complexities. The inferolateral and pterygoid recesses (11%) add intricacy to the tapestry of skull base vulnerabilities. The suprasellar cell is part of the posterior group of frontal recess cells, distinct from the frontal bullae cell. Frontal cells are categorised into types 1 to 4, with a modified classification including both type 3 and 4 cells as frontal cells that pneumatised through the frontal sinus ostium. The presence of a pedicled ethmoidal artery often correlates with hyperpneumatized ethmoidal cells (7).

**Anatomy and Considerations of the Anterior Skull Base in ESS :**The anterior skull base is formed by the cribriform plate medially and the ethmoidal roof laterally. Keros classified the skull base into three types based on the depth of the olfactory groove. The anterior skull base slopes downward posteriorly, making it crucial to dissect low during endoscopic sinus surgery (ESS). The anterior ethmoidal artery (AEA) lies posterior to the frontal recess, usually within the skull base, but can be pedicled or slinging downward within a mesentery. Preoperative CT scans can identify low-lying ethmoidal arteries (8). The modern era of ESS began in the 1950s, with Messerklinger's work on endoscopic anatomy and the emphasis on the ostiomeatal complex's role in rhinosinusitis. ESS is now the primary approach for chronic rhinosinusitis, with external and nonendoscopic methods having limited indications. The AEA's position in the ethmoid sinus is highly variable, placing it at risk during ESS. Its relationship with the skull base is crucial, as injury

risk increases when it lies freely below it. Understanding the relevant anatomy and its variations is essential before any ESS procedure (9,10).

**Computed Tomography (CT) in Rhinosinusitis Imaging and Identifying the AEA :** CT is the standard for rhinosinusitis evaluation due to its ability to differentiate between hypertrophic mucosa, bone, and air. It also complements MRI for tumour evaluation and guides surgical navigation. Multichannel CT scanners provide thin slices and quick evaluations but use ionising radiation, which poses long-term risks. Iodinated contrast is not typically needed for rhinosinusitis evaluation. The AEA lies posterior to the frontal recess, usually enclosed in the skull base, but can sometimes be pedicled or slinging downward within the ethmoidal space. Preoperative CT scans can identify low-lying ethmoidal arteries. Anatomical landmarks for identifying the AEA include the bony notch on the medial wall of the orbit and the bone sulcus on the lateral wall of the olfactory fossa (11).

## Material and Methods

**Study Design:** This study investigated the radiological and endoscopic features of anatomical landmarks that localise the anterior ethmoidal artery (AEA) in endoscopic sinus surgery. It was a prospective case-control study conducted from June 2021 to May 2022. The institutional review board approved the study of the Arab Board of Health Specializations.

**Study Setting:** The study was conducted at Sulaymaniyah Teaching Hospital/otolaryngology-head and Neck Surgery Center and the Middle East ENT Center in Zhyan Private Hospital.

**Participants:** The study included patients who underwent functional endoscopic sinus surgery (FESS) to treat chronic rhinosinusitis (CRS) that was resistant to maximal medical therapy. The patients were selected based on inclusion and exclusion criteria.

**Inclusion Criteria:**

- Patients undergoing bilateral FESS for reluctant CRS

- Complete demographic, radiological, and operative data available

- Consent to participate in the study

**Exclusion Criteria:**

- Patients with incomplete data

- Age less than 16 years old

- Patients undergoing revision FESS

- Patients with benign and malignant nasal and paranasal tumours

**Data Collection:** Demographic, radiological, and operative data were collected for each included patient. Demographic data, including name, age, and sex, were recorded. Radiological data were obtained from CT scans using a standard MSCT Scanner (Siemens) with a bone algorithm. The scans' slice thickness was 2 mm or less. The DICOM radiant viewer software was used to review the CT scans and reconstruct them into three-dimensional views.

**Anatomical Landmarks:** Several anatomical landmarks were studied and reviewed on the CT scans to determine their relation with the location of the anterior ethmoidal artery. These landmarks included:

**Supraorbital ethmoid cell (SOEC):** The SOEC was defined as the ethmoid cell immediately posterior and lateral to the frontal ostium with lateral pneumatisation of the orbital plate of the frontal bone beyond the plane of the most medial portion of the lamina papyracea. Coronal and axial views were utilised to define the SOEC.

**Suprabullar cell (SBC):** The SBC is the anterior ethmoidal cell between the ethmoid bullae and the skull base. SBC pneumatisation was determined using sagittal views to identify the second lamella (ethmoid bulla) attachment to the skull base.

**Olfactory Fossa depth:** The depth of the olfactory fossa was measured at the level of the cribriform plate's first appearance in the coronal plane. The vertical height of the lateral lamella was measured from the cribriform plate plane to the level of the fovea. This measurement categorised the fossa depth into Keros types I, II, and III.

**Anterior ethmoidal artery:** The AEA was identified by observing the lamina papyracea and the anterior ethmoidal foramen on the coronal view of the CT scan. Several parameters were used to identify the AEA, including the globe's disappearance, the medial rectus and superior oblique muscles on the superomedial border of the orbit, and Kennedy's nipple. The distance between the AEA and the skull base was measured on a coronal section.

**Operative Videos:** Operative videos of the included patients were reviewed to correlate the endoscopic findings regarding the site of the AEA within or below the skull base with the radiological notes of the presence of the SOEC, SBC, and the site of the anterior ethmoidal artery.

**Surgical Technique:** All patients underwent FESS following a standard technique. The surgical procedure included bunionectomy, middle meatal antrostomy (MMA), anterior-posterior ethmoidectomy (APE), sphenoidotomy, and frontal sinus draft IIa and IIb. Nasal patties mixed with a decongestant solution prepared the nasal cavity, and surgery proceeded with laminectomy and subsequent steps.

**Statistical Analysis:** Data analysis was performed using the Statistical Package for Social Sciences (SPSS) program version 22. Frequency and percentages were used to describe qualitative data, while mean and standard deviation were used for quantitative data. The chi-square test was

used to determine associations between categorical data. A p-value of 0.05 or less was considered statistically significant.

**Results :**Based on the data presented in Figure (1), out of the 50 patients, 30 were male, accounting for 60% of the sample, while 20 were female, representing 40%. Additionally, Table 1 presents the age distribution of the FESS patients. The table reveals that the patients' ages ranged from 18 to 73.

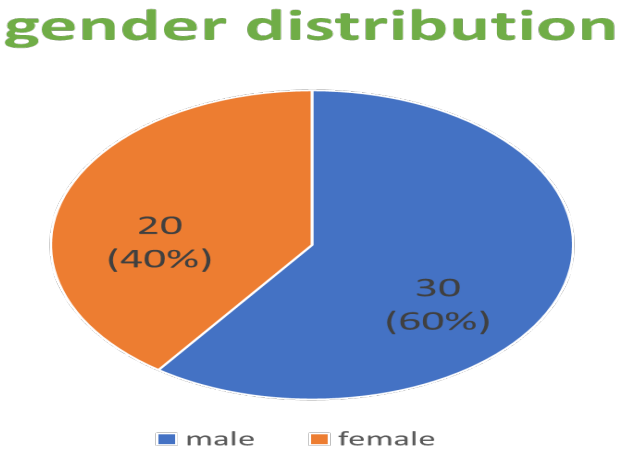


**Figure (1): gender distribution**

**Table (1): The age distribution**

| | N | Minimum | Maximum | Mean | Std. Deviation |
|---|---|---|---|---|---|
| **Age** | **50** | **17** | **73** | **39.22** | **12.505** |
| **Valid N (Listwise)** | **50** | | | | |

Table (2) shows various anatomical variations observed in a sample of 50 individuals, comprising 20 females (40%) and 30 males (60%). Regarding the presence of supra-orbital cells, the right side showed 26 cases (52%) with absence and 24 cases (48%) with presence, while the left side had 22 cases (44%) with absence and 28 cases (56%) with presence. For the supra-bullar cells, the right side had 11 cases (22%) with absence and 39 cases (78%) with presence, whereas the left side had 17 cases (34%) with absence and 33 cases (66%) with presence. The KEROS classification, which describes the depth of the olfactory fossa, showed the following distribution: on the right side, 31 cases (62%) were Type 1, 19 cases (38%) were Type 2, and 0 cases (0%) were Type 3; on the left side, 27 cases (54%) were Type 1, 23 cases (46%) were Type 2, and 0 cases (0%) were Type 3. The anatomical position of the anterior ethmoidal artery (AEA) was also evaluated. On the right

side, 32 cases (64%) had the AEA within the skull base, while 18 cases (36%) had it below it. On the left side, 27 cases (54%) had the AEA within the skull base, and 23 cases (46%) had it below it.

**Table (2): Anatomical variabilities:**

| | | Frequency | Per Cent |
|---|---|---|---|
| **Gender** | **Female** | **20** | **40.0** |
| | **Male** | **30** | **60.0** |
| **Rt. Supra Orb. Cell** | **Absent** | **26** | **52.0** |
| | **Presence** | **24** | **48.0** |
| **Lt. Supra Orb. Cell** | **Absent** | **22** | **44.0** |
| | **Presence** | **28** | **56.0** |
| **Rt. Supra Bullar Cell** | **Absent** | **11** | **22.0** |
| | **Presence** | **39** | **78.0** |
| **Lt. Supra Bullar Cell** | **Absent** | **17** | **34.0** |
| | **Presence** | **33** | **66.0** |
| **Rt. KEROS** | **Type 1** | **31** | **62.0** |
| | **Type 2** | **19** | **38.0** |
| | **Type 3** | **0** | **0** |
| **Lt. KEROS** | **Type 1** | **27** | **54.0** |
| | **Type 2** | **23** | **46.0** |
| | **Type 3** | **0** | **0** |
| **Rt. AEA (Radiological)** | **Within Skull Base** | **32** | **64.0** |
| | **Below Skull Base** | **18** | **36.0** |
| **Lt. AEA (Radiological)** | **Within Skull Base** | **27** | **54.0** |
| | **Below Skull Base** | **23** | **46.0** |
| **Total** | | **50** | **100.0** |

Table 3 comprehensively analyses the relationship between anatomical structures and the right-sided anterior ethmoid artery (AEA) location relative to the skull base. The data is examined statistically, providing counts, percentages, and p-values. The table examines three essential structures: the supra-orbital ethmoid cell (SOEC), the supra-bullar cell (SBC), and the Keros types. For each structure, contingency tables show the counts and percentages when they are absent or present within or below the skull base. The SOEC shows a strong relationship ($p \leq 0.001$) between its presence/absence and AEA location, while the SBC does not ($p=0.149$). The distribution of Keros types is also explored, with Type 1 being the most common (75%).

**Table (3): Relationship of the SOEC, SBC and Keros types with the AEA coarse level at the Rt side(radiologically)**

| | | | Rt. AEA (radiological) | | Total | P- Value |
|---|---|---|---|---|---|---|
| | | | Within Skull Base | Below Skull Base | | |
| Rt. Supra Orb. Cell | Absent | Count | 23 | 3 | 26 | ≤ 0.001 |
| | | % | 71.9% | 16.7% | 52.0% | |
| | Presence | Count | 9 | 15 | 24 | |
| | | % | 28.1% | 83.3% | 48.0% | |
| Rt. Supra Bullar Cell | Absent | Count | 9 | 2 | 11 | 0.149 |
| | | % | 28.1% | 11.1% | 22.0% | |
| | Presence | Count | 23 | 16 | 39 | |
| | | % | 71.9% | 88.9% | 78.0% | |
| Rt. KEROS | Type 1 | Count | 24 | 7 | 31 | 0.013 |
| | | % | 75.0% | 38.9% | 62.0% | |
| | Type 2 | Count | 8 | 11 | 19 | |
| | | % | 25.0% | 61.1% | 38.0% | |
| | Type 3 | count | 0 | 0 | 0 | |
| Gender | Female | Count | 13 | 7 | 20 | 0.574 |
| | | % | 40.6% | 38.9% | 40.0% | |
| | Male | Count | 19 | 11 | 30 | |
| | | % | 59.4% | 61.1% | 60.0% | |
| Total | | Count | 32 | 18 | 50 | |
| | | % | 100.0% | 100.0% | 100.0% | |

Table (4) examines three essential structures: the supra-orbital ethmoid cell (SOEC), the supra-bullar cell (SBC), and the Keros types. The SOEC and Keros types show strong relationships ($p \leq 0.001$ and $p=0.002$, respectively) between their presence/absence and AEA location, while the SBC shows a more moderate association ($p=0.022$). The distribution of Keros types is also explored, with Type 1 being the most common (74.1%).

**Table (4): Relationship Of The SOEC, SBC And Keros Types With The AEA Coarse Level At The Lt Side(Radiologically)**

| | | | Lt. AEA (Radiologically) | | Total | P- Value |
|---|---|---|---|---|---|---|
| | | | Within Skull Base | Below Skull Base | | |
| Lt. Supra Orb. Cell | Absent | Count | 19 | 3 | 22 | ≤ 0.001 |
| | | % | 86.4% | 13.6% | 100.0% | |
| | Presence | Count | 8 | 20 | 28 | |
| | | % | 28.6% | 71.4% | 100.0% | |
| Lt. Supra Bullar Cell | Absent | Count | 13 | 4 | 17 | 0.022 |
| | | % | 76.5% | 23.5% | 100.0% | |
| | Presence | Count | 14 | 19 | 33 | |
| | | % | 42.4% | 57.6% | 100.0% | |
| Lt. Keros | Type 1 | Count | 20 | 7 | 27 | 0.002 |
| | | % | 74.1% | 25.9% | 100.0% | |
| | Type 2 | Count | 7 | 16 | 23 | |
| | | % | 30.4% | 69.6% | 100.0% | |
| | Type 3 | Count | 0 | 0 | 0 | |
| Gender | Female | Count | 12 | 8 | 20 | 0.343 |
| | | % | 60.0% | 40.0% | 100.0% | |
| | Male | Count | 15 | 15 | 30 | |
| | | % | 50.0% | 50.0% | 100.0% | |
| Total | | Count | 27 | 23 | 50 | |
| | | % | 54.0% | 46.0% | 100.0% | |

Based on the data presented in Table (5), the SOEC and Keros types show strong relationships ($p \leq 0.001$ and $p=0.013$, respectively) between their presence/absence and AEA location. In contrast, the SBC shows no significant association ($p=0.149$). The distribution of Keros types is also explored, with Type 1 being the most common (75.0%).

**Table (5): Relationship of The SOEC, SBC And Keros Types With The AEA Coarse Level At The Rt Side (Endoscopically)**

| | | | Rt. AEA (By Endoscopy) | | Total | P- Value |
|---|---|---|---|---|---|---|
| | | | Within Skull Base | Below Skull Base | | |
| Rt. Supra Orb. Cell | Absent | Count | 23 | 3 | 26 | ≤ 0.001 |
| | | % | 71.9% | 16.7% | 52.0% | |
| | Presence | Count | 9 | 15 | 24 | |
| | | % | 28.1% | 83.3% | 48.0% | |
| Rt. Supra Bullar Cell | Absent | Count | 9 | 2 | 11 | 0.149 |
| | | % | 28.1% | 11.1% | 22.0% | |
| | Presence | Count | 23 | 16 | 39 | |
| | | % | 71.9% | 88.9% | 78.0% | |
| Rt. KEROS | Type 1 | Count | 24 | 7 | 31 | 0.013 |
| | | % | 75.0% | 38.9% | 62.0% | |
| | Type 2 | Count | 8 | 11 | 19 | |
| | | % | 25.0% | 61.1% | 38.0% | |
| Gender | Female | Count | 13 | 7 | 20 | 0.574 |
| | | % | 40.6% | 38.9% | 40.0% | |
| | Male | Count | 19 | 11 | 30 | |
| | | % | 59.4% | 61.1% | 60.0% | |
| Total | | Count | 32 | 18 | 50 | |
| | | % | 100.0% | 100.0% | 100.0% | |

According to the data presented in Table (6), the Lt. AEA data shows that 19 occurrences (86.4%) were within the skull base, and three occurrences (13.6%) were below the skull base. The p-value for this relationship is ≤ 0.001. The Lt. Supra Orb. Cell data indicates that eight occurrences (28.6%) were absent, and 20 occurrences (71.4%) were present. The Lt. Supra Bullar Cell data shows that 13 occurrences (76.5%) were lacking, and four occurrences (23.5%) were present, with a p-value of 0.022. The Lt. Keros Type 1 and Type 2 data show that 20 occurrences (74.1%) were Type 1, and 7 occurrences (25.9%) were Type 2, with a p-value of 0.002. The gender data indicates that 12 occurrences (60.0%) were female, and eight occurrences (40.0%) were male, with a p-

value of 0.343. The total count for the table is 50 occurrences (100.0%), with 27 occurrences (54.0%) falling into one category and 23 occurrences (46.0%) falling into another category, with a p-value of 10, which does not hold statistical significance.

**Table ( 6): Relationship Of The SOEC, SBC And Keros Types With The AEA Coarse Level At The Lt Side(Endoscopically)**

| | | | Lt. AEA (Endoscopy) | | Total | P- Value |
|---|---|---|---|---|---|---|
| | | | Within Skull Base | Below Skull Base | | |
| Lt. Supra Orb. Cell | Absent | Count | 19 | 3 | 22 | ≤ 0.001 |
| | | % | 86.4% | 13.6% | 100.0% | |
| | Presence | Count | 8 | 20 | 28 | |
| | | % | 28.6% | 71.4% | 100.0% | |
| Lt. Supra Bullar Cell | Absent | Count | 13 | 4 | 17 | 0.022 |
| | | % | 76.5% | 23.5% | 100.0% | |
| | Presence | Count | 14 | 19 | 33 | |
| | | % | 42.4% | 57.6% | 100.0% | |
| Lt. Keros | Type 1 | Count | 20 | 7 | 27 | 0.002 |
| | | % | 74.1% | 25.9% | 100.0% | |
| | Type 2 | Count | 7 | 16 | 23 | |
| | | % | 30.4% | 69.6% | 100.0% | |
| Gender | Female | Count | 12 | 8 | 20 | 0.343 |
| | | % | 60.0% | 40.0% | 100.0% | |
| | Male | Count | 15 | 15 | 30 | |
| | | % | 50.0% | 50.0% | 100.0% | |
| Total | | Count | 27 | 23 | 50 | |
| | | % | 54.0% | 46.0% | 100.0% | |

Table 7 presents the vertical distance of the anterior ethmoidal artery (AEA) from the skull base when the AEA is located below the skull base, separately for the right and left sides. The table provides the average (mean) distance for each side, with 2.998mm for the right side and 2.966mm for the left side. Furthermore, the table does not include statistical tests to evaluate the significance of any observed differences.

| **Table (7) :Shows The Vertical Distance Of The AEA From The Skull Base In Cases Where The AEA Were Below The Skull Base.** | | |
|---|---|---|
| | **Right Side** | **Left Side** |
| **The Vertical Distance Of The AEA From The Skull Base At Mid-Point** | **From 1.5mm-4.8mm** | **1.5mm-4.92mm** |
| **The Average** | **2.998mm** | **2.966mm** |

As shown in Figure (2), the P values for SBC and the type of Keros were significant for the AEA course, and the P value for SOEC was substantial for the course of AEA both radiologically and endoscopically.

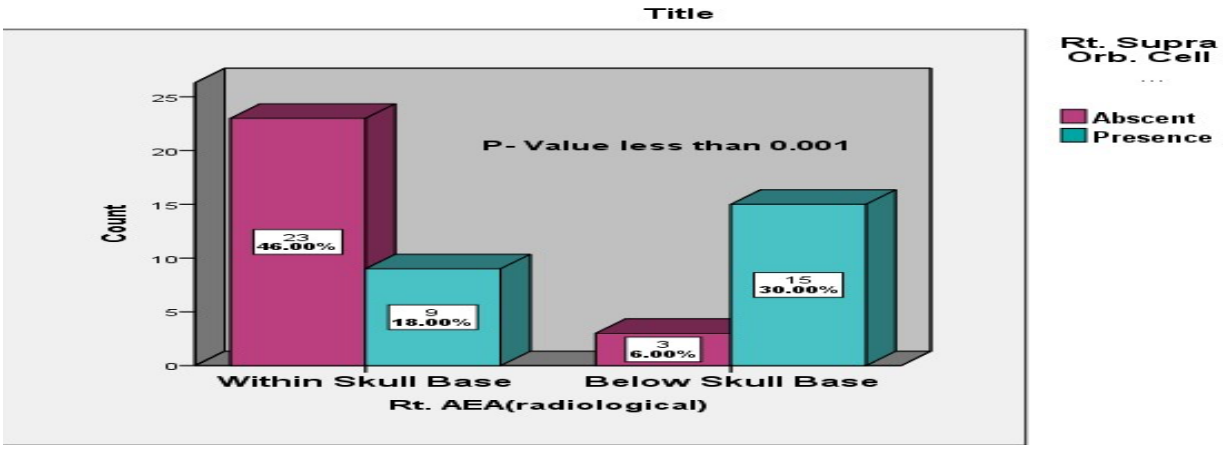


Figure (2): Association between Rt. AEA with Rt. Supra Orbital cell

The data presented in Figure 3 shows the association between the left anterior ethmoid artery (Lt. AEA) and the left supraorbital cell, as observed endoscopically. The figure depicts a scatter plot with Lt. AEA on the x-axis and the left supraorbital cell on the y-axis. The data points appear to exhibit a positive correlation, indicating that as the value of the Lt. AEA increases, the value of the left supraorbital cell also tends to increase.

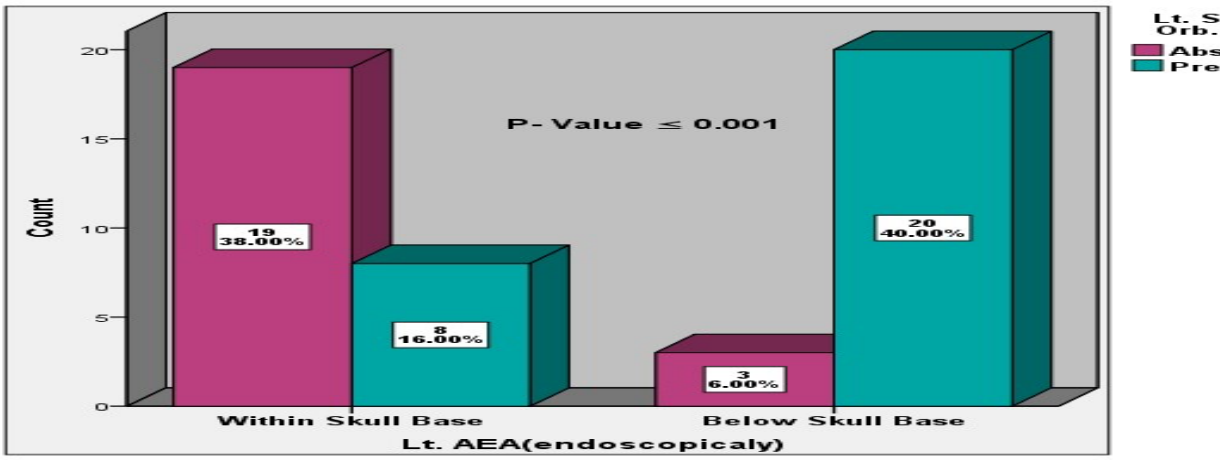


Figure (3): Association between Lt. AEA (Endoscopically) with Lt. Supra Orbital cell

Table 8 presents statistical data on the association between the right (Rt) and left (Lt) anterior ethmoidal artery (AEA). It provides counts and percentages for different categories based on the AEA's location relative to the skull base. The table is divided into three main sections: "Within Skull Base," "Below Skull Base," and "Total." Each section includes counts and percentages for the Lt AEA and Rt AEA. In the "Within Skull Base" section, there were 23 occurrences (71.9%) where the Lt AEA was within the skull base, while nine occurrences (28.1%) were below the skull base. The calculated p-value for this association is < 0.001, indicating a statistically significant relationship between the Lt AEA and its position relative to the skull base. Similarly, for the Rt AEA within the skull base, 32 occurrences (100.0%) were reported. No occurrences were reported below the skull base for the Rt AEA. Moving to the "Below Skull Base" section, there were four occurrences (22.2%) where the Lt AEA was below the skull base, while 14 occurrences (77.8%) were within the skull base. For the Rt AEA below the skull base, there were 18 occurrences (100.0%), indicating that all instances were located below the skull base. Finally, the "Total" section provides the overall counts and percentages for the Lt AEA and Rt AEA. Of the 50 occurrences, 27 (54.0%) were associated with the Lt AEA, and 23 (46.0%) were related to the Rt AEA.

Table (8): Association between Rt and Lt AEA.

| | | | Lt. AEA | | Total | P Value |
|---|---|---|---|---|---|---|
| | | | Within Skull Base | Below Skull Base | | |
| Rt. AREA | Within Skull Base | Count | 23 | 9 | 32 | < 0.001 |
| | | % | 71.9% | 28.1% | 100.0% | |
| | Below Skull Base | Count | 4 | 14 | 18 | |
| | | % | 22.2% | 77.8% | 100.0% | |
| Total | | Count | 27 | 23 | 50 | |
| | | % | 54.0% | 46.0% | 100.0% | |

The data presented in Figure 4 shows the association between Rt (right) and Lt (left) AEA (anterior ethmoidal artery). The figure depicts a scatter plot with Rt AEA on the x-axis and Lt AEA on the y-axis. The data points appear to form a positive linear relationship, indicating that as the value of Rt AEA increases, the value of Lt AEA also tends to increase.

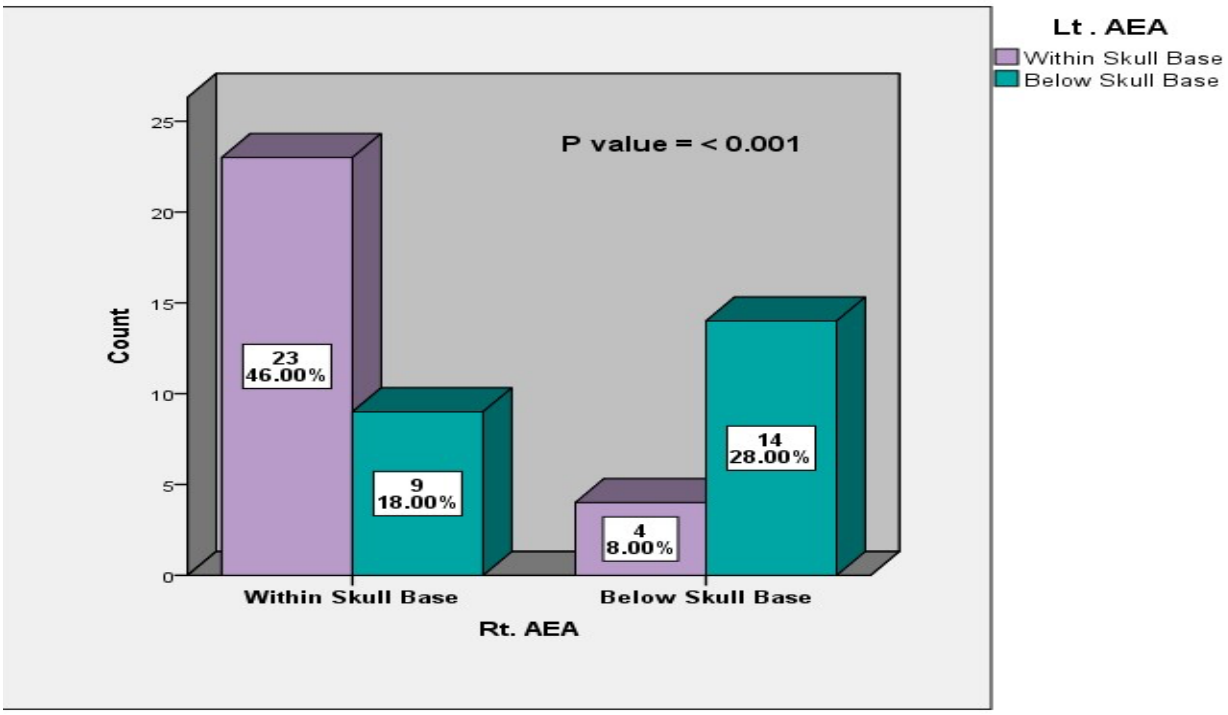


Figure (4): association between Rt and Lt AEA.

## Discussion

The AEA, a branch of the ophthalmic artery, follows a complex and variable path through multiple cavities before reaching the nasal cavity, including the orbit, ethmoidal roof, and anterior cranial fossae. If not accurately identified, the AEA's course poses a risk of injury during ESS, with potential complications such as CSF leakage from medial injury or retroorbital hematoma and optic nerve compression from lateral injury. Preoperative CT scans are crucial for determining the AEA's trajectory, while intraoperative identification is essential to prevent accidental damage during ESS. In their study of 76 patients undergoing PNS CT scans, Li et al. (12) found that the presence of SOEC was linked not only to a higher occurrence of the AEA coursing below the skull base across all Keros types but also to an increased distance below the skull base. Consequently, this raises the vulnerability of the artery to injury during ESS. In a study conducted by Joshi et al. (13) on 50 randomly selected PNS CT scans, they investigated the occurrence of the AEA below the skull base and the impact of SOEC presence on the vertical distance between the artery and the skull base. The results revealed that the mean distance between the artery and the skull base was 1.5 mm in the absence of the supraorbital cell, whereas it increased to 2.5 mm when the cell was present. This difference was statistically significant ($p = 0.000$), indicating a high significance level.

In a study by Simmen et al. (14), 34 cadaveric heads were dissected and subjected to coronal, axial, and sagittal CT scans to identify the AEA's location. Among these specimens, 10 exhibited extensive pneumatisation of the SOEC, with the AEA observed at an average distance of 3.7 mm below the skull base. On the other hand, in 6 specimens with limited SOEC pneumatisation, the artery was only 0.2 mm away from the skull base. Among the remaining 18 specimens, where no SOEC was present, all had the AEA within the skull base, except for one where the artery was below the skull base. This study reveals that when the SOEC is present on the right side, 83.3% of the cases exhibit the AEA below the skull base within a bony mesentery on that same side. Similarly, when the SOEC is present on the left side, 71.4% of the cases show the AEA situated below the skull base on the corresponding side. These findings strongly indicate a significant association between the presence of SOEC and the presence of the AEA below the skull base, as observed in both radiological and endoscopic studies of the AEA (P value ≤0.001, highly significant) and based on these findings revealed that a heightened susceptibility of the AEA to injury during ESS.

A study conducted by Poteet et al. (15) investigated the correlation between the location of the AEA and Keros classification. The study included 101 patients who underwent PNS or maxillofacial CT scans. Among the participants, 54 were female (53.5%) and 47 were male (46.5%). Each side was evaluated as a separate measurement in the study. Our investigation revealed exciting findings regarding the right side. Among cases where the depth of the olfactory fossa was classified as type 1 Keros, we observed that 38.9% of them demonstrated the AEA below the skull base. At the same time, most had an artery within the skull base. However, for cases where the olfactory fossa depth was classified as type 2 Keros, an astonishing 61.1% displayed the AEA positioned below the skull base. These results imply a notable positive correlation between the length of the LLCP and the presence of the AEA below the skull base on the same side. This correlation was statistically significant, with a P value of 0.013.

In our analysis of the left side, we found intriguing results. When the depth of the olfactory fossa was categorised as type 1 Keros, we observed that 25.9% of the cases exhibited the AEA positioned below the skull base. At the same time, most had an artery within the skull base. However, when the olfactory fossa depth was classified as type 2 Keros, 69.6% displayed the AEA below the skull base. These findings suggest a significant favourable influence of the length of the LLCP on the AEA, which is located below the skull base on the same side. The statistical analysis indicated a P value of 0.002, indicating a solid significance level.

In their study, Umar et al. (16) highlight the importance of investigating the effects of suprasellar pneumatisation on the orientation of surrounding anatomical structures relevant to the frontal drainage pathway. The findings revealed a significant correlation between the type of suprasellar pneumatisation and the course of the AEA along the skull base ($p = 0.04$), as well as the position of the AEA at the second lamella ($p = 0.04$). As the grading of suprasellar pneumatisation

increased, the AEA was projected to have a lower position at the skull base and be situated at a greater distance from the second lamella. In our current investigation, we made noteworthy observations on the right side. When the supraorbital cell (SBC) was present, a striking 88.9% of the cases exhibited the presence of the AEA below the skull base. On the contrary, when the SBC was absent, only 11.1% of the cases showed the AEA below the skull base. These findings suggest a significant impact of the SBC's presence on the course of the AEA within the ethmoid labyrinth, causing it to be situated below the skull base. However, the statistical analysis yielded a P value of 0.149, indicating a lack of statistical significance. Similarly, on the left side, in the presence of the SBC, we observed that 57.6% of the cases displayed the presence of the AEA below the skull base. Conversely, when the SBC was absent, only 23.5% of the cases had the AEA positioned below the skull base. These results indicate a significant influence of the SBC's presence on the course of the AEA within the ethmoid labyrinth, leading to its location below the skull base. The statistical analysis in this case yielded a P value of 0.022, suggesting statistical significance.

## Conclusion

A thorough examination of ESS patients necessitates comprehensive radiological CT scans to assess the presence of SOEC and SBC pneumatisation, LLCP length, and Keros classification. SOEC pneumatisation significantly influences the trajectory of the AEA, with a greater likelihood of it passing below the skull base if SOEC is present. Determining LLCP length and the presence of SBC pneumatisation are equally important, as they also impact the AEA's course relative to the skull base. This meticulous evaluation is essential for preventing inadvertent AEA injuries, which may result in severe complications such as blindness and CSF leaks if the artery is retracted towards the orbit or cribriform plate and anterior skull base.

## Limitation

A small sample size and anatomical and ethnic variability limit the study. Additionally, the radiological assessment did not evaluate the degree of SOEC pneumatisation or the type of SBC pneumatisation. Moreover, the vertical distance was not considered when assessing the coarse level of the AEA from the skull base. Furthermore, neither the radiological nor endoscopic assessments evaluated the location of the AEA about the attachment of the skull base-ethmoidal lamellae.

## References

1. Abdullah B, Lim EH, Husain S, Snidvongs K, Wang DY. Anatomical variations of anterior ethmoidal artery and their significance in endoscopic sinus surgery: a systematic review. Surgical and Radiologic Anatomy. 2019 May.

2. Yuresh Naidoo and P.J. Wormald. Endoscopic and Open Anterior/ Posterior Ethmoid Artery Ligation. In: CHIU AG, PALMER JN, ADAPPA ND, editors. Atlas of endoscopic sinus and skull base surgery. Second edition. | Philadelphia, PA: Elsevier; 2019. P.25-26.

3. Dustin M Dalgorf and Richard J. Harvey. ANATOMY OF THE NOSE AND PARANASAL

SINUSES. In: Watkinson JC, Clarke RW, editors. Scott-Brown's otorhinolaryngology and head and neck surgery: Volume 1: Basic sciences, endocrine surgery, rhinology. EIGHTH EDITION. CRC Press; 2018 Jun 12. P. 974-975

4. Devyani Lal, James A. Stankiewicz. Primary Sinus Surgery. In: Flint PW, Francis HW, Haughey BH, Lesperance MM, Lund VJ, Robbins KT, Thomas JR, editors. Cummings Otolaryngology Head and Neck Surgery. Seventh edition. Philadelphia, PA 19103-2899: Copyright © 2021 by Elsevier Inc. P. 677-678.

5. Devyani Lal, James A. Stankiewicz. Primary Sinus Surgery. In: Flint PW, Francis HW, Haughey BH, Lesperance MM, Lund VJ, Robbins KT, Thomas JR, editors. Cummings Otolaryngology Head and Neck Surgery. Seventh edition. Philadelphia, PA 19103-2899: Copyright © 2021 by Elsevier Inc. P. 684-686.

6. Devyani Lal, James A. Stankiewicz. Primary Sinus Surgery. In: Flint PW, Francis HW, Haughey BH, Lesperance MM, Lund VJ, Robbins KT, Thomas JR, editors. Cummings Otolaryngology Head and Neck Surgery. Seventh edition. Philadelphia, PA 19103-2899: Copyright © 2021 by Elsevier Inc. P. 684.

7. Almushayti ZA, Almutairi AN, Almushayti MA, Alzeadi HS, Alfadhel EA, AlSamani AN.

Evaluation of the Keros Classification of Olfactory Fossa by CT Scan in Qassim Region. Cureus. 2022 Feb 19;14(2).

8. Bonasia S, Smajda S, Ciccio G, Robert T. Anatomic and Embryologic Analysis of the Dural Branches of the Ophthalmic Artery. American Journal of Neuroradiology. 2021 Mar 1;42(3):414416.

9. Majid Khan, S. James Zinreich, Nafi Aygun. Imaging of Nose and Sinuses. . In: Flint PW, Francis HW, Haughey BH, Lesperance MM, Lund VJ, Robbins KT, Thomas JR, editors. Cummings Otolaryngology Head and Neck Surgery. Seventh edition. Philadelphia, PA 191032899: Copyright © 2021 by Elsevier Inc. P. 616.

10. Philip R. Chapman. NOSE AND SINUS.In: Koch BL,Hamilton BE, Hudgins PA, Harnsberger HR, editors. Diagnostic imaging Head and Neck. Third Edition. 1600 John F. Kennedy Blvd. Ste 1800 Philadelphia, PA 19103-2899: Elsevier; 2017. P. 666-667.

11. Baban MI, Hadi M, Gallo S, Zocchi J, Turri-Zanoni M, Castelnuovo P. Radiological and clinical interpretation of the patients with CSF leaks developed during or after endoscopic sinus surgery. European Archives of Oto-Rhino-Laryngology. 2017 Jul;274(7):2827-35.

12. Li M, Sharbel DD, White B, Y. Tadros S, Kountakis SE. Reliability of the supraorbital ethmoid cell vs Keros classification in predicting the course of the anterior ethmoid artery. InInternational Forum of Allergy & Rhinology 2019 Jul (Vol. 9, No. 7, pp. 821-824).

13. Joshi AA, Shah KD, Bradoo RA. Radiological correlation between the anterior ethmoidal artery and the supraorbital ethmoid cell. Indian Journal of Otolaryngology and Head & Neck Surgery. 2010 Sep;62(3):299-303.

14. Simmen D, Raghavan U, Briner HR, Manestar M, Schuknecht B, Groscurth PJ, Jones NS. The surgeon's view of the anterior ethmoid artery. Clin otolaryngol. 2006 Jun 1;31(3):187-91.

15. Poteet PS, Cox MD, Wang RA, Fitzgerald RT, Kanaan A. Analysis of the relationship between the location of the anterior ethmoid artery and Keros classification. Otolaryngology– Head and Neck Surgery. 2017 Aug;157(2):320-4.

16. Umar NF, Aziz ME, Mat Lazim N, Abdullah B. The Effects of Suprabullar Pneumatization on the Orientation of Its Surrounding Anatomical Structures Relevant to the Frontal Drainage Pathway. Diagnostics. 2021 Dec 27;12(1):52.